Physics Letters A 175 (1993) 133–137
North-Holland

PHYSICS LETTERS A

Charge asymmetry of ionization cross sections of atomic hydrogen by antiproton and proton impact

Nobuyuki Toshima
Institute of Applied Physics, University of Tsukuba, Tsukuba, Ibaraki 305, Japan

Received 3 December 1992; revised manuscript received 9 February 1993; accepted for publication 10 February 1993
Communicated by B. Fricke

Large-scale coupled-channel calculations are carried out for the evaluation of the ionization cross section of atomic hydrogen by antiproton impact. The dependence of the ionization cross sections on the projectile charge is investigated in comparison with the case of proton impact. It is demonstrated that continuum states of the antiproton, which were not taken into account satisfactorily in previous calculations, play an important role for the ionization. The ionization cross section ratio of the antiproton and proton impact obtained by the present coupled-channel calculations is close to the classical trajectory Monte Carlo (CTMC) value at variance with the result of Ermolaev [Phys. Lett. A 149 (1990) 151].

Since the first-order Born cross sections for the ionization of a hydrogen atom by a naked ion do not depend on the sign of the projectile charge, the difference of the cross sections by antiproton and proton impact arises solely from higher-order perturbations. Hence the study of the charge asymmetry of the ionization cross sections gives direct information on the effect of higher-order interactions.

Ermolaev [1] calculated the ionization cross section $\sigma(\bar{p})$ of atomic hydrogen by antiproton impact by means of the coupled-channel method and compared it with the ionization cross section $\sigma(p)$ by proton impact. The ratio $\sigma(\bar{p})/\sigma(p)$ of the quantal calculation was different from the result of the classical trajectory Monte Carlo (CTMC) calculation [2]. The quantal ratio shows weaker energy-dependence than the classical one in the velocity range $1<v<5$ a.u. though the behavior bears some qualitative similarity. On the other hand, in a larger velocity range of $5<v<11$ a.u. the quantal curve shows a broad maximum exceeding unity by 7% while the classical ratio is almost constant and always smaller than unity. These discrepancies might imply that the classical description of the ionization process is not adequate in the intermediate energy region and higher-order effects which are missing in the classical treatment are not negligible in the MeV region. However, it is not justified to attribute the discrepancies totally to the failure of the classical description of ionization processes without a check of the convergence of the coupled-channel calculations.

Recently Toshima and Eichler [3,4] successfully extended the coupled-channel method to the study of the Thomas mechanism [5] expanding high-lying continuum states by Gauss-type orbitals (GTO). They have shown that high-lying continuum states which have the same average electron velocity as the relative motion of the nuclei (matching-velocity state) are selectively populated in the projectile and play a decisive role in the Thomas double scattering as well as the target continuum states. Following their study, Toshima [6] demonstrated that the enhanced population of the high-lying continuum states of the projectile is not only a characteristic of the Thomas process but also a general feature of the high-energy ion–atom collisions. Though it is known that both target and projectile continuum states are required at lower energies for representing the molecular nature of the electronic states induced by the two-center forces [7], it has not been well realized that the ionization processes of the target atom are also affected by the presence of the projectile continuum states even at high energies. In fact, only one continuum state was attached to the projectile for the

antiproton impact and no continuum state was used in the projectile for the case of proton impact in the calculations of Ermolaev [1].

In this Letter, we calculate the ionization cross sections of the processes

$$\bar{p}+H(1s)\rightarrow\bar{p}+p+e\,, \tag{1}$$

$$p+H(1s)\rightarrow p+p+e \tag{2}$$

using the coupled-channel method employing a large number of continuum states both in the target and in the projectile. The relative motion of the heavy particles is described classically by a rectilinear trajectory with a constant velocity $\boldsymbol{v}$ in the impact-parameter representation. The time-dependent two-center electronic wave function is expanded as

$$\Psi(\boldsymbol{r},t)=\sum_{i=1}^{N_T} a_i(t)\psi_i^T(\boldsymbol{r}_T,t)+\sum_{i=N_T+1}^{N} a_i(t)\psi_i^P(\boldsymbol{r}_P,t) \tag{3}$$

in terms of the target functions

$$\psi_i^T(\boldsymbol{r}_T,t)=\varphi_i^T(\boldsymbol{r}_T)\exp(-iE_i^T t) \tag{4}$$

and the projectile functions

$$\psi_i^P(\boldsymbol{r}_P,t)=\varphi_i^P(\boldsymbol{r}_P)\exp(-iE_i^P t)\times\exp(i\boldsymbol{v}\cdot\boldsymbol{r}_T)\exp(-\tfrac{1}{2}iv^2 t)\,. \tag{5}$$

Here, $\boldsymbol{r}_T$, $\boldsymbol{r}_P$ are the electron coordinates measured from the target and projectile nucleus, respectively, and φ_i^T, φ_i^P are the eigenfunctions of the target and projectile Hamiltonian with eigenvalues E_i^T and E_i^P.

We further expand the eigenfunctions of each center in terms of Gauss-type basis functions as

$$\varphi_{nlm}(\boldsymbol{r})=\sum_{\nu} c_\nu^{(nl)}\exp(-\alpha_\nu r^2)r^l Y_{lm}(\hat{\boldsymbol{r}})\,, \tag{6}$$

where the nonlinear parameters α_ν are generated as a modified geometrical progression in the interval $2.5\times10^{-3}\leqslant\alpha_\nu\leqslant400$. The coefficients c_ν^{nl} are determined so as to diagonalize the atomic Hamiltonian of the target and the projectile [3,4]. The quantization axis of the atoms is chosen to be perpendicular to the collision plane. By this choice the whole basis set is uncoupled into two subsets with even or odd symmetry for mirror reflection with respect to the collision plane. Since the initial state has even symmetry, we need to couple only states with $l+m=$ even. The numbers of GTO and diagonalized eigenstates used for the expansion in the energy range below 100 keV are listed in table 1. The physical eigenstates obtained after diagonalization cover the energy range from -0.5 to 100 a.u. The highest state is chosen to be higher than twice the matching-velocity state, and hence the total number of states is increased as the collision energy increases above 100 keV. The eigenenergies of the hydrogen bound states have an accuracy of 10^{-6} to 10^{-7}.

The coupled-channel code used for the present calculations was originally designed for the study of the Thomas double-scattering process [3,4]. Since the probability of the double-scatterings is extremely small, a highly precise calculation was required to prevent the small probability of 10^{-10} from being embedded under the numerical inaccuracy. In the GTO expansion all the matrix elements can be evaluated analytically, and it is possible to get matrix elements as accurately as desired in contrast with the standard method based on the Slater-type orbital (STO) expansion in which numerical integration is required for two-center matrix elements. The STO expansion is not suitable for ionization processes in high-energy collisions because the convergence of the numerical integration becomes quickly worse as the number of nodes of the wave function increases or the oscillation induced by the electron-translation factor becomes serious. We have calculated the matrix elements at 250 points in the half space $t\leqslant0$ and converted those to the region $t>0$ using the reflection rule [4]. This number of points is sufficiently large to get accurate matrix elements at any point by interpolation. The accuracy of the numerical calcu-

Table 1
The numbers of GTO and diagonalized eigenstates used for the expansion of each angular-momentum l below 100 keV. The real number of basis functions is to be multiplied by $l+1$, the multiplicity of the magnetic quantum numbers for $l+m=$even

l	Proton		Antiproton	
	GTO	eigenstates	GTO	eigenstates
0	20	10	15	10
1	16	9	12	9
2	13	6	9	6
3	9	6	8	6
4	8	4	8	4

lations for solving the large-basis coupled equations is checked carefully by changing the mesh intervals to obtain sufficient convergence. The validity of unitarity and detailed balancing was also used as a measure of the numerical accuracy. In general, calculations for ionization processes are much easier than for electron-capture processes since the probability of ionization does not decrease quickly as the collision energy increases.

The cross section ratios $\sigma(\bar{p})/\sigma(p)$ for processes (1) and (2) are plotted in fig. 1. The present coupled-channel cross section ratio is closer to the classical value [2] than to the quantal result of Ermolaev [1]. We show individual cross sections and the parts of ionization into the target and projectile continuum states separately in table 2. It is evident that the difference between the two quantal results arises mainly from the contribution of the projectile continuum states. The partial cross sections for the ionization into the target continuum states are not strongly dependent on the sign of the projectile charge except for the lowest collision energy whereas the partial cross sections for ionization into the projectile continuum states depend considerably on the projectile charge below 200 keV. It is interesting to note that the partial ratio of the cross sections into target continuum states only is close to the results of Ermolaev below 500 keV. Ermolaev's ratio exceeds 1.0 above 500 keV and takes a maximum value of 1.07 around 1500 keV. The present cross section ratio exceeds 1.0 only slightly at the highest two energies.

No experimental data is available for the ionization of atomic hydrogen by antiproton impact. The experimental data for a helium-atom target [8] and a molecular-hydrogen target [9] do not show the hump found by Ermolaev around 1 MeV. At lower energies the experimental ratio $\sigma(\bar{p})/\sigma(p)$ differs from unity by about 20% for helium and about 15% for molecular hydrogen. However, it is not justified to apply these values of atomic hydrogen directly because the effects of the electron–electron correlation and of the molecular structure become important for low-energy collisions. The experimental data for ionization of atomic hydrogen by proton impact [10] are normalized to the Born cross section at 1.5 MeV. It was demonstrated in a previous paper that the coupled-channel cross sections show a deviation from the Born approximation values even in the MeV region, and questions were raised respecting the normalization procedure of the experimental data [6]. Though the cross sections of Ermolaev [1] are a little closer to the experimental values normalized to the Born cross section than ours, the present cross sections become closer instead if the measured values are normalized to our cross section at 1.5 MeV.

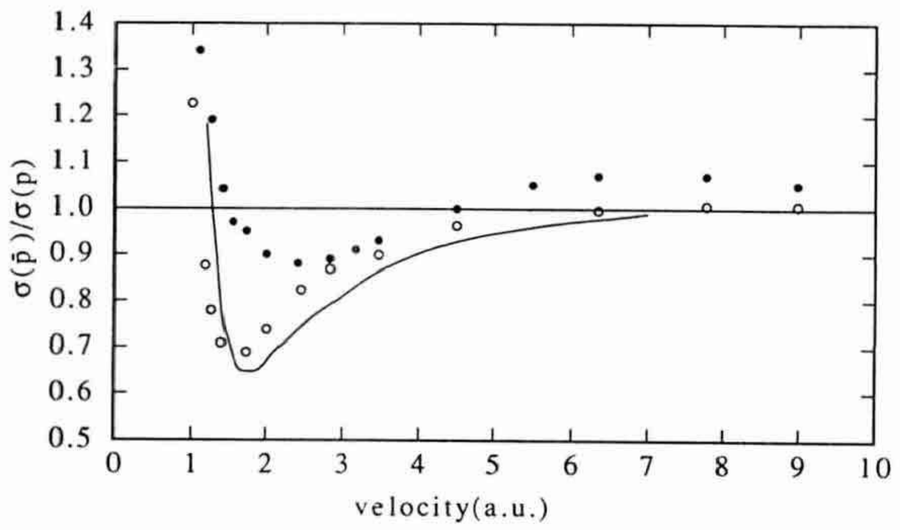

Fig. 1. The ratio of the ionization cross sections of atomic hydrogen by antiproton and proton impact. (○) Present coupled-channel calculations; (●) results of Ermolaev [1]. (—) CTMC results of Schultz [2].

Table 3 gives the partial cross sections for ionization into the individual angular momentum states at 50 and 1500 keV. The distribution of the target continua has a peak at $l=1$ as can be expected from the dominance of the optically allowed transitions. As the collision energy increases, the dominance of the $l=1$ states becomes more prominent. On the contrary, the distribution of the projectile continua has a peak at $l=0$ for low energy collisions and it tends to become flatter at high energies. The present ionization cross sections for proton impact are generally larger than the values of Shakeshaft [11], who also studied the ionization of atomic hydrogen by the coupled-channel method using pseudocontinuum states on both the target and projectile. The difference from our results comes mainly from the contribution of $l=3$ and 4 states, which were not included in the calculation of Shakeshaft. The number of pseudostates with $l\leqslant 2$ in his calculation is also smaller than the number used in the present study.

The projectile continuum states are required even for the antiproton which interacts with the electron repulsively. They are necessary to make more complete the description of the electron-cloud distribution repelled by the antiproton. In this sense the ion-

Table 2
Ionization cross sections of atomic hydrogen by proton and antiproton impact in units of 10^{-17} cm^2 and their ratio. T and P denote the parts of the ionization into the target and projectile continuum states, respectively. The cross sections for proton impact at 200, 500, 1000, 1500 and 2000 keV are from ref. [6]

E (keV)	v (a.u.)	$\sigma(\mathrm{p})$			$\sigma(\bar{\mathrm{p}})$			$\sigma(\bar{\mathrm{p}})/\sigma(\mathrm{p})$		
		T	P	total	T	P	total	T	P	total
25	1.00	5.33	8.00	13.33	10.30	6.04	16.34	1.932	0.755	1.226
35	1.19	8.29	9.16	17.45	10.52	4.77	15.28	1.268	0.521	0.876
40	1.27	8.43	10.64	19.07	10.51	4.35	14.86	1.246	0.409	0.779
50	1.42	9.56	10.15	19.70	10.02	3.93	13.94	1.048	0.388	0.708
75	1.74	9.66	7.62	17.27	9.03	2.88	11.91	0.935	0.378	0.689
100	2.01	10.11	4.71	14.82	9.06	1.85	10.91	0.897	0.393	0.737
150	2.46	7.87	2.69	10.56	7.26	1.43	8.69	0.922	0.533	0.823
200	2.84	7.25	1.46	8.70	6.61	0.94	7.55	0.913	0.644	0.868
300	3.48	5.05	0.89	5.94	4.69	0.65	5.34	0.928	0.732	0.899
500	4.49	3.34	0.58	3.92	3.18	0.59	3.77	0.953	1.026	0.964
1000	6.35	2.00	0.31	2.30	1.93	0.37	2.29	0.965	1.203	0.997
1500	7.78	1.40	0.23	1.63	1.36	0.28	1.64	0.973	1.221	1.007
2000	8.98	1.10	0.15	1.25	1.08	0.19	1.26	0.978	1.214	1.007

Table 3
Cross sections for ionization into each partial wave in units of cm^2 at 50 and 1500 keV. T and P denote the parts of the ionization into the target and projectile continuum states, respectively. $a(b)$ denotes $a\times10^b$.

l	50 keV				1500 keV			
	p impact		$\bar{\mathrm{p}}$ impact		p impact		$\bar{\mathrm{p}}$ impact	
	T	P	T	P	T	P	T	P
0	1.32(−17)	6.67(−17)	6.52(−18)	1.79(−17)	7.27(−19)	6.23(−19)	6.93(−19)	8.38(−19)
1	3.95(−17)	2.11(−17)	5.15(−17)	1.06(−17)	1.01(−17)	5.59(−19)	9.94(−18)	8.61(−19)
2	2.64(−17)	7.44(−18)	2.74(−17)	4.92(−18)	2.21(−18)	4.55(−19)	2.08(−18)	5.76(−19)
3	1.09(−17)	3.35(−18)	1.02(−17)	3.08(−18)	7.73(−19)	3.60(−19)	6.93(−19)	3.16(−19)
4	5.51(−18)	2.87(−18)	4.55(−18)	2.79(−18)	2.04(−19)	2.61(−19)	1.78(−19)	1.67(−19)
total	9.56(−17)	1.02(−16)	1.00(−16)	3.93(−17)	1.40(−17)	2.26(−18)	1.36(−17)	2.76(−18)

ization into the antiproton continuum is essentially different from the so-called *capture to the continuum* (CTC) component of positive ions. The latter denotes the component of free electrons that follow the projectile with the same speed being attracted by the interaction from the projectile. In the case of proton impact, the CTC component makes a significant contribution at low energies but the contribution decreases rapidly as the collision energy increases in accordance with the results of Crothers and McCann [12]. Instead the high-lying continuum states around the velocity-matching energy give a dominant contribution among the projectile continuum states there. The component of the high-lying projectile continuum states is also different from the CTC component of electrons since the CTC component has small relative kinetic energies if the electrons are seen from the projectile.

In summary we have shown that projectile continuum states are important for the description of the ionization of target atomic hydrogen for antiproton impact as well as for proton impact. The inclusion of the projectile continuum states makes the asymmetry of the ionization cross section for antiproton and proton impact larger at low energies and, on the contrary, smaller at high energies.

References

[1] A.M. Ermolaev, Phys. Lett. A 149 (1990) 151; J. Phys. B 23 (1990) L45.
[2] D.R. Schultz, Phys. Rev. A 40 (1989) 2330.
[3] N. Toshima and J. Eichler, Phys. Rev. Lett. 66 (1991) 1050.
[4] N. Toshima and J. Eichler, Phys. Rev. A 46 (1992) 2564.
[5] R. Shakeshaft and L. Spruch, Rev. Mod. Phys. 51 (1979) 369.
[6] N. Toshima, J. Phys. B 25 (1992) L635.
[7] W. Fritsch and C.D. Lin, Phys. Rep. 202 (1991) 1.
[8] L.H. Andersen, P. Hvelplund, H. Knudsen, S.P. Møller, J.O.P. Pedersen, S. Tang-Petersen, E. Uggerhøj, K. Elsener and E. Morenzoni, Phys. Rev. A 41 (1990) 6536.
[9] L.H. Andersen, P. Hvelplund, H. Knudsen, S.P. Møller, J.O.P. Pedersen, S. Tang-Petersen, E. Uggerhøj, K. Elsener and E. Morenzoni, J. Phys. B 23 (1990) L395.
[10] M.B. Shah and H.B. Gilbody, J. Phys. B 14 (1981) 2361; M.B. Shah, D.S. Elliot and H.B. Gilbody, J. Phys. B 20 (1987) 2481.
[11] R. Shakeshaft, Phys. Rev. A 18 (1978) 1930.
[12] D.S.F. Crothers and J.F. McCann, J. Phys. B 16 (1983) 3229.